Soft Matter

RSC Publishing

PAPER

Self-healing hydrogels formed in catanionic surfactant solutions†‡

Cite this: *Soft Matter*, 2013, **9**, 2254

Gizem Akay,[a] Azadeh Hassan-Raeisi,[b] Deniz C. Tuncaboylu,[c] Nermin Orakdogen,[a] Suzan Abdurrahmanoglu,[d] Wilhelm Oppermann*[b] and Oguz Okay*[a]

Received 1st November 2012
Accepted 11th December 2012

DOI: 10.1039/c2sm27515e

www.rsc.org/softmatter

Physical gels with remarkable properties were obtained by copolymerization of acrylamide with the hydrophobic monomer stearyl methacrylate (C18) in a micellar solution of cetyltrimethylammonium bromide (CTAB) containing up to 15 mol% sodium dodecyl sulfate (SDS). The addition of SDS causes the CTAB micelles to grow and thus enables solubilization of C18. The gels exhibit time-dependent dynamic moduli, high elongation ratios at break (1800–5000%), and self-healing, as evidenced by rheological and mechanical measurements and substantiated by dynamic light scattering. As the size of the micelles in the gelation solution increases, both the degree of temporary spatial inhomogeneity and the lifetime of hydrophobic associations in the gels increase while the elongation ratio at break decreases. Although the physical gels were insoluble in water due to strong hydrophobic interactions, they could be solubilized in surfactant solutions thus providing a means of characterization of the network chains. Viscometric and rheological behaviors of polymer solutions show a substantial increase in the associativity of the network chains with rising micelle size, which results in prolonged lifetime of hydrophobic associations acting as physical cross-links in gels. The internal dynamics of self-healing gels could thus be controlled by the associativity of the network chains which in turn depends on the size of CTAB micelles.

Introduction

Synthetic hydrogels are very similar to biological tissues and, therefore, have received considerable attention for use in tissue engineering, drug release, soft contact lenses, sensors, and actuators.[1] One disadvantage of such hydrogels is mechanical weakness and lack of ability to self-heal, which hinders their use in many application areas. This poor mechanical performance mainly originates from their very low resistance to crack propagation due to the lack of an efficient energy dissipation mechanism in the chemically cross-linked polymer network.[2–5] To obtain self-healing gels with a high degree of toughness, one has to increase the overall viscoelastic dissipation by creating a polymer network where cross-linking occurs *via* reversible breakable cross-links with finite lifetimes, instead of permanent cross-links.[6–12] Numerous studies have been conducted in recent years to improve the mechanical performance of hydrogels.[13–22]

Recently, we presented a simple strategy to generate strong hydrophobic interactions between hydrophilic polymers leading to the production of self-healing hydrogels.[23] Large hydrophobes such as stearyl methacrylate (C18) or docosyl acrylate (C22) could be copolymerized with the hydrophilic monomer acrylamide (AAm) in a micellar solution of sodium dodecyl sulfate (SDS). This was achieved by the addition of a salt into the reaction solution. Salt leads to micellar growth[24–26] and thus enables solubilization of large hydrophobes within the grown wormlike SDS micelles. After their solubilization and after incorporation of the hydrophobic sequences within the hydrophilic polymer chains *via* a micellar polymerization technique,[27–33] strong hydrophobic interactions can be generated in synthetic hydrogels. It was shown that the hydrophobic associations between the polymer chains prevent dissolution in water and flow, while the dynamic nature of the junction zones provides homogeneity and self-healing properties together with a high degree of toughness.[23,34] However, drastic structural changes were observed when SDS micelles were removed from the physical gels.[34] Several dynamic characteristics of the gels

[a]*Department of Chemistry, Istanbul Technical University, 34469 Istanbul, Turkey. E-mail: okayo@itu.edu.tr; Fax: +90-2122856386; Tel: +90-2122853156*

[b]*Institute of Physical Chemistry, Clausthal University of Technology, 38678 Clausthal-Zellerfeld, Germany. E-mail: wilhelm.oppermann@tu-clausthal.de; Fax: +49-5323-722863; Tel: +49-5323-722205*

[c]*Faculty of Pharmacy, Bezmialem Vakif University, 34093 Istanbul, Turkey. E-mail: dtuncaboylu@bezmialem.edu.tr; Fax: +90-2125332326; Tel: +90-2125232288*

[d]*Department of Chemistry, Marmara University, 34722 Istanbul, Turkey. E-mail: suzana@marmara.edu.tr; Fax: +90-2163478783; Tel: +90-2163451186*

† This paper is dedicated to the late Prof. Ayhan Demir (1950–2012), a distinguished organic chemist and Editor-in-Chief of the *Turkish Journal of Chemistry*.

‡ Electronic Supplementary Information (ESI) available: ICFs and $G(\Gamma)$'s of surfactant solutions; swelling kinetics of gels; zero-shear viscosities for polymer solutions. See DOI: 10.1039/c2sm27515e

including their self-healing behavior completely vanish after extraction of SDS micelles, indicating the loss of the reversible nature of the cross-linkages. These findings suggest that the presence of a surfactant is critically important for the unique properties of self-healing hydrogels formed by hydrophobic associations.

An alternative route to promote micellar growth is mixing of surfactants of opposite charges. Aqueous mixtures of cationic and anionic surfactants, called catanionic surfactants, exhibit unique properties and several types of microstructures arising from the strong electrostatic interactions between the oppositely charged head groups. Depending on the concentration and composition of surfactant systems, temperature, and salt addition, they form mixed micelles, vesicles, lamellar phases, precipitates, spheres, or rod-like structures.[35–41] Mixtures of the anionic surfactant SDS and the cationic surfactant cetyltrimethylammonium bromide (CTAB) form mixed micelles in both SDS-rich and CTAB-rich solutions while between these compositions, vesicles and formation of a 1 : 1 precipitate are observed.[42–45]

Here, we prepared physical polyacrylamide (PAAm) hydrogels by micellar copolymerization of AAm with 2 mol% C18 in aqueous CTAB–SDS solutions. Since the Krafft point for CTAB in water was reported to be around 20–25 °C,[46] both the gelation reactions and the characterization of the physical gels were carried out at 35 °C. The surfactant and the initial monomer concentrations during gelation were set to 0.24 M and 5 w/v%, respectively. We first investigated the growth of CTAB micelles upon addition of SDS in the CTAB-rich region up to the onset of turbidity. Simultaneously, the solubilization extent of C18 was determined in dependence on the size of the mixed micelles. The micellar copolymerization reactions were then carried out and the physical gels formed were characterized by dynamic light scattering, rheological and mechanical measurements. As will be shown below, the internal dynamics of self-healing gels are controlled by the associativity of the network chains, which in turn depends on the size of CTAB micelles. The results also show that replacement of SDS–NaCl with a CTAB–SDS mixed micellar system further improves the mechanical performance of self-healing hydrogels.

Experimental part

Materials

Acrylamide (AAm, Merck), cetyltrimethylammonium bromide (CTAB, Sigma), sodium dodecylsulfate (SDS, Merck), ammonium persulfate (APS, Sigma-Aldrich), and *N*,*N*,*N*′,*N*′-tetramethylethylenediamine (TEMED, Sigma) were used as received. Commercially available stearyl methacrylate (C18, Aldrich) consists of 65% *n*-octadecyl methacrylate and 35% *n*-hexadecyl methacrylate. An APS stock solution was prepared by dissolving 0.8 g APS in 10 mL of distilled water. 0.24 M stock solutions of each of the surfactants were prepared by dissolving 4.373 g CTAB and 3.460 g SDS separately in 50 mL water at 35 °C. CTAB–SDS solutions of various compositions were prepared by mixing these stock solutions at 35 °C to obtain a final volume of 10 mL. In accordance with previous works,[42–45] we observed that the surfactant solutions became opaque if the SDS content was between 20 and 70 mol% while homogeneous and transparent solutions were obtained outside of this concentration range. We conducted the gelation reactions in CTAB-rich regions of the solutions, *i.e.*, in 0.24 M CTAB–SDS solutions containing 0 to 15 mol% SDS.

Hydrogel preparation

Micellar copolymerization of AAm with C18 was conducted at 35 °C in the presence of an APS (3.5 mM)–TEMED (0.25 v/v%) redox initiator system. Following parameters were fixed:

Total monomer (acrylamide + C18) concentration: 5 w/v%.

Hydrophobe content of the monomer mixture: 2 mol%.

Total surfactant (CTAB + SDS) concentration: 0.24 M.

To illustrate the synthetic procedure, we give details of the preparation of hydrogels in CTAB–SDS solutions containing 15 mol% SDS. An SDS stock solution (1.50 mL) was mixed with a CTAB stock solution (8.50 mL) at 35 °C to obtain a transparent solution. Then, C18 (0.044 g) was dissolved in this CTAB–SDS solution under stirring for 2 h at 35 °C. After addition and dissolving acrylamide (0.456 g) for 30 min, TEMED (25 μL) was added into the solution. Finally, 100 μL of an APS stock solution was added to initiate the reaction. A portion of this solution was transferred between the plates of the rheometer to follow the reaction by oscillatory small-strain shear measurements and to perform additional rheological experiments. For the dynamic light scattering measurements, the solution was filtered through Nylon membrane filters with a pore size of 0.2 μm into light scattering vials. The remaining part of the solution was transferred into several plastic syringes of 4.65 mm internal diameters and the polymerization was conducted for one day at 35 °C.

Quantification of the solubilization of C18 in CTAB–SDS solutions

The amount of C18 solubilized in the micelles was estimated by measuring the transmittance of CTAB–SDS solutions containing various amounts of C18 at 35 °C on a T80 UV-visible spectrophotometer. The transmittance at 500 nm was plotted as a function of the added amount of C18 in the CTAB–SDS solution and, the solubilization extent of C18 was determined by the curve break.

Rheological experiments

Gelation reactions were carried out at 35 °C within the rheometer (Gemini 150 Rheometer system, Bohlin Instruments) equipped with a cone-and-plate geometry with a cone angle of 4° and diameter of 40 mm. The instrument was equipped with a Peltier device for temperature control. During all rheological measurements, a solvent trap was used to minimize the evaporation. The reactions were monitored at an angular frequency ω of 6.3 rad s^{-1} and a deformation amplitude $\gamma_o = 0.01$. After a reaction time of 5 h, the dynamic moduli of the reaction solutions approached limiting values. Then, frequency-sweep tests and stress-relaxation experiments were carried out at 35 °C, as described before.[23]

Dynamic light scattering (DLS) measurements

DLS measurements were performed at 35 °C using an ALV/CGS-3 compact goniometer (ALV, Langen, Germany) equipped with a cuvette rotation/translation unit (CRTU) and a He–Ne laser (22 mW, $\lambda = 632.8$ nm). Details about the instrument have been described before.[23] The scattering angle θ was varied between 50° and 130° corresponding to scattering vector amplitudes $q = (4\pi n/\lambda)\sin(\theta/2)$ between 1.1×10^7 and 2.4×10^7 m^{-1}. Several time average intensity correlation functions $g_T^{(2)}(q,\tau)$ (ICF) of the physical gels were acquired applying exceptionally long measuring times of 2 hours, while for most experiments the acquisition time was limited to 100 s allowing sampling of 100 different positions selected by randomly moving the CRTU before each run.

When such position dependent measurements had been made, the partial heterodyne method was applied to divide the time-averaged scattering intensity into its two components:[47–49]

$$\langle I(q)\rangle_T = I_C(q) + \langle I_F(q)\rangle_T \quad (1)$$

where $I_C(q)$ and $\langle I_F(q)\rangle_T$ are the scattering intensities due to the frozen structure and liquid-like concentration fluctuations, respectively. This procedure also gave the cooperative diffusion coefficient D.

For ergodic media like surfactant solutions, the scattering intensity contains only a fluctuating component and is independent of the sample position. $g_T^{(2)}(q,\tau)$ is then equivalent to an ensemble-averaged intensity correlation function and can be written as the Laplace transform of the distribution of relaxation rates, $G(\Gamma)$ (we disregard a coherence factor):

$$g_T^{(2)}(q,\tau) - 1 = \left[\int_0^\infty G(\Gamma)\exp(-\Gamma\tau)\mathrm{d}\Gamma\right]^2 \quad (2)$$

where Γ is the characteristic relaxation rate. $G(\Gamma)$ values at five angles (50°, 70°, 90°, 110°, and 130°) were evaluated with an inverse Laplace transform of $g_T^{(2)}(q,\tau) - 1$ with the integrated ALV software (Fig. S1‡). Relaxation rates of the fast (Γ_{fast}) and slow modes (Γ_{slow}) were obtained from the peak values of Γ in $G(\Gamma)$s. The hydrodynamic correlation length ξ_H was evaluated using the Stokes–Einstein relation:

$$\xi_H = \frac{kT}{6\pi\eta D} \quad (3)$$

where η is the viscosity of the medium (0.72 mPa s^{-1}) and kT is the Boltzmann energy.

Uniaxial elongation measurements

The measurements were performed on cylindrical hydrogel samples of about 4.6 mm diameter at 31.0 ± 0.5 °C on a Zwick Roell test machine using a 10 N load cell under the following conditions: crosshead speed = 50 mm min^{-1}, sample length between jaws = 14 ± 2 mm. The tensile strength and percentage elongation at break were recorded. For reproducibility, 11 samples were measured for each gel and the results were averaged.

Gel fractions and swelling measurements

Cylindrical hydrogel samples (diameter: 4.65 mm, length: about 2 cm) were immersed in a large excess of water at 35 °C for at least 15 days by replacing water every day to extract any soluble species. The masses m of the gel samples were monitored as a function of swelling time by weighing the samples. Relative weight swelling ratio m_{rel} of gels was calculated as $m_{rel} = m/m_0$, where m_0 is the initial mass of the gel sample. Then, the equilibrium swollen gel samples with relative masses $m_{rel,eq}$ were taken out of water and freeze dried. The gel fraction W_g, that is, the conversion of monomers to the water-insoluble polymer (mass of cross-linked polymer/initial mass of the monomer) was calculated from the masses of dry, extracted polymer network and from the comonomer feed.

Solubilization of gels and characterization of network chains

Although the physical gels formed by the associations of C18 blocks were insoluble in water, they could be solubilized in surfactant solutions. The following procedure was applied in the solubilization experiments: the gel sample (1 g) at the state of preparation was immersed into 10 mL of a 0.24 M CTAB–SDS solution at 35 °C and shaken for a duration of 3 days until complete solubilization. The composition of the external CTAB–SDS solution was the same as that of the surfactant solution in the gel sample. The solution thus obtained with a polymer concentration of 0.5 w/v% was then subjected to frequency-sweep tests at $\gamma_o = 0.01$ and viscosity measurements at various shear rates between 10^{-3} and 10^3 s^{-1}.

Results and discussion

The micellar copolymerization of AAm with 2 mol% C18 was carried out at 35 °C in 0.24 M CTAB–SDS solutions of various SDS contents between 0 and 15 mol%. In the following, we will first discuss the growth of CTAB micelles upon addition of SDS, allowing solubilization of the hydrophobe C18 in the gelation solutions. Then, dynamic and mechanical properties of the self-healing gels formed by the micellar copolymerization will be discussed with regard to the size of mixed micelles. This section also deals with the characterization of the associative properties of the network chains isolated from the gels, which will explain the results of our observations.

Gelation solutions

The structural changes in CTAB micelles induced by the addition of SDS were investigated at 35 °C by DLS measurements. The CTAB solution exhibits both fast and slow relaxation modes that merge into one upon addition of 15 mol% SDS (Fig. S1 and S2‡). This behavior is similar to that of polyelectrolyte solutions after addition of a salt.[50] In Fig. 1A, the relaxation rate of the fast mode (Γ_{fast}) is plotted against q^2 for 0.24 M CTAB–SDS solutions of various compositions between 0 and 15% SDS. Γ_{fast} is proportional to q^2 indicating the existence of diffusive processes in the surfactant solutions. Most notably, the relaxation rates decrease markedly with rising SDS content in the surfactant mixture, obviously because of the growth of the micelles.

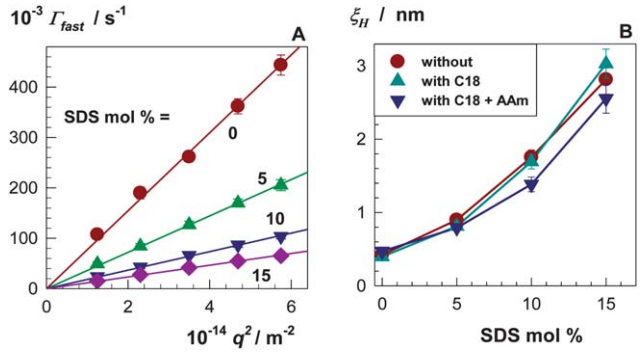

Fig. 1 (A): Relaxation rate of the fast mode (Γ_{fast}) plotted against q^2 for 0.24 M CTAB–SDS solutions with various SDS contents. Temperature = 35 °C. (B): Hydrodynamic correlation length ξ_H of 0.24 M CTAB–SDS solutions with or without the monomers plotted against the SDS content of the micellar solution.

Since the relaxation rate Γ of a particular mode is related to the diffusion coefficient D as $\Gamma = Dq^2$, we calculated D of the micelles from the slope of Γ_{fast} *versus* q^2 plots and the corresponding hydrodynamic correlation length ξ_H using the Stokes–Einstein relation (eqn (3)). In Fig. 1B, ξ_H is plotted against the SDS content of CTAB–SDS solutions before and after addition of the monomers C18 and AAm. While the correlation length ξ_H increases with rising SDS content, it does not change significantly upon addition of the monomers. This behavior is substantially different from that of wormlike SDS micelles formed in NaCl solutions in which the micelles change their shape from cylindrical to spherical after solubilization of the hydrophobes,[51–55] so that ξ_H decreases.[23]

Increasing size of the micelles also increased the solubility of the hydrophobic comonomer C18 in the micellar solution. Fig. 2A shows the transmittance T at 500 nm of CTAB–SDS solutions at 35 °C as a function of the amount of C18 added. In the absence of SDS, T starts to decrease at 0.3% C18, indicating the appearance of insolubilized C18 particles in the solution, while with rising amount of SDS in the micellar solution, this decrease starts at higher C18 concentrations. In Fig. 2B, the solubilization extent of C18 determined by the curve break is plotted against the SDS content of CTAB–SDS solutions. In parallel with increasing size of the micelles (Fig. 1B), C18 solubility also increases with rising SDS content of the solutions. The dashed horizontal line in the figure representing the amount of C18 used in the micellar polymerization reveals that C18 could be completely solubilized in CTAB–SDS solutions so that a comonomer composition with 2 mol% C18 is realized. However, in a pure CTAB solution, only 2/3 of C18 is soluble, *i.e.*, the comonomer mixture in the micellar solution will contain 1.4 mol% C18. We note that, in contrast to the partial solubilization of C18 in a 0.24 M CTAB solution, it is insoluble in a 0.24 M SDS solution.[23] The larger solubilization power of CTAB micelles is attributed to its larger aggregation number and longer alkyl chain length as compared to SDS micelles.[42]

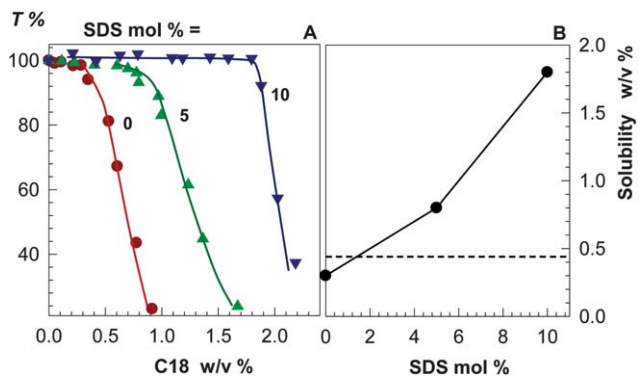

Fig. 2 (A): Transmittance T at 500 nm of aqueous 0.24 M CTAB–SDS solutions plotted against the amount of C18 added. SDS content as indicated. Temperature = 35 °C. (B): Solubility of C18 in CTAB–SDS solutions plotted against SDS content. The dashed line indicates the C18 concentration used in the experiments (0.44 w/v%).

Dynamics of physical gels

After addition of the monomers and the initiator into the micellar solution and after completion of the copolymerization reactions, physical gels were obtained in the whole range of SDS contents studied. Both the gelation solutions and the physical gels were transparent as long as the temperature remained above the Krafft point of CTAB (~25 °C), while they became cloudy at lower temperatures. Therefore, all measurements were conducted at 35 °C.

Fig. 3A shows an example of the time average intensity correlation function (ICF) obtained with a measurement time of 2 hours at $\theta = 90°$ on a gel formed with 15% SDS. It exhibits two relaxation modes: a major fast one at 40 μs and a minor one smeared out over several decades of time in the range 1–1000 s. When the DLS measurements were performed as usual with

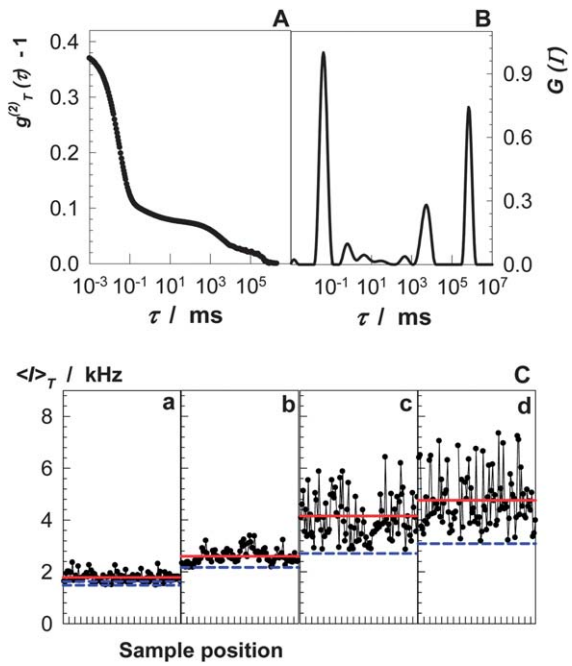

Fig. 3 (A and B): ICF and distribution of relaxation times $G(\Gamma)$ obtained with a measurement time of 2 h at $\theta = 90°$ on a gel formed with 15 mol% SDS. Temperature = 35 °C. (C): Variation of $\langle I \rangle_T$ at $\theta = 90°$ with hundred different sample positions for gels formed at 0 (a), 5 (b), 10 (c) and 15 mol% SDS (d). Measurement time per position = 100 s.

measurement times around 100 s, the longer relaxations are lost or erroneously appear at shorter times. The CONTIN analysis of the ICF reveals the distribution of relaxation times displayed in Fig. 3B: The longest relaxation time peaks at 700 s ($\approx$12 min) indicating very slow dynamics in such gels. We think that these long relaxations are characteristic of the temporary nature of the network.

When the measuring time is chosen to be appreciably shorter than the longest relaxation time, the system behaves like a permanent gel that could be simply recognized by observing speckles, *i.e.*, random fluctuations in the intensity of scattered light as a function of sampling position. Fig. 3C shows such variations of time-averaged scattering intensity $\langle I\rangle_T$ for gels with SDS contents between 0 and 15%. These data were obtained with a measurement time per position of 100 s at $\theta = 90^\circ$. The solid lines represent the ensemble-averaged scattering intensity, $\langle I\rangle_E$, while the dashed lines represent the scattering intensities $\langle I_F\rangle_T$ due to liquidlike concentration fluctuations. $\langle I\rangle_T$ $\langle I\rangle_E$ for all gels indicates inhomogeneity on a short time scale: 100 s are far too short for the gel to explore the whole configuration space. $\langle I_F\rangle_T$ monotonically increases with rising SDS content due to the fact that an appreciable portion of the thermal scattering in these gels is due to the presence of large CTAB–SDS mixed micelles. The static component (frozen structure) of the scattered intensity, $I_C/\langle I\rangle_E$, increases from 10 to 30 % with rising SDS content indicating that the gel inhomogeneity increases as the micelles grow bigger. This increase is possibly related to the increasing lifetime of the hydrophobic associations acting as physical cross-links (see below). Visual observations indeed showed that the gels formed without or with 5% SDS were too weak while those formed at higher SDS contents were relatively strong.

Rheological measurements are another means of studying the dynamic properties of the gels. Fig. 4A shows the frequency dependencies of the elastic modulus G' (filled symbols) and viscous modulus G'' (open symbols) for the gels with varying SDS contents. In Fig. 4B, the relaxation moduli $G(t)$ of the same gels in the linear regime, obtained from stress relaxation measurements, are plotted against time t at different strains γ_o. The gels exhibit frequency- or time-dependent dynamic moduli indicating the temporary nature of the hydrophobic associations having lifetimes of the order of seconds to milliseconds, with $G'(\omega)$ being a mirror image of $G(t)$. At time scales over 2 decades (1–100 s), they exhibit a power-law behavior, $G(t) \propto t^{0.31 \pm 0.08}$, as indicated by the solid red lines. At times shorter than 1 s, a Rouse-type relaxation is seen which was fitted using the stretched exponential function $G(t) = G_R\exp(-(t/\tau_1)^\beta)$ with an exponent $\beta = 0.46 \pm 0.04$, where G_R is the Rouse modulus and τ_1 is the lifetime of associations, *i.e.*, the average residence time of a hydrophobic block in a given association (dashed red curves in the figures).[20,56–58]

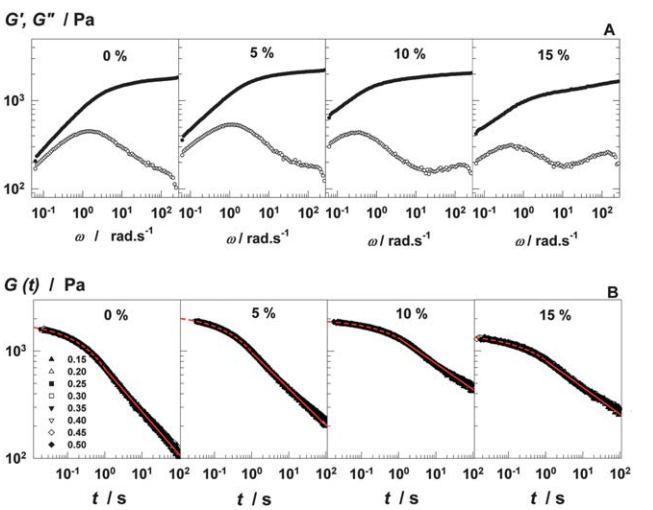

Fig. 4 (A): G' (●) and G'' (○) of gels shown as a function of angular frequency ω. $\gamma_o = 0.01$. SDS amounts in CTAB–SDS mixtures (in mol%) are indicated. Temperature = 35 °C. (B): The relaxation modulus $G(t)$ of gels as a function of time t for various strains γ_o indicated.

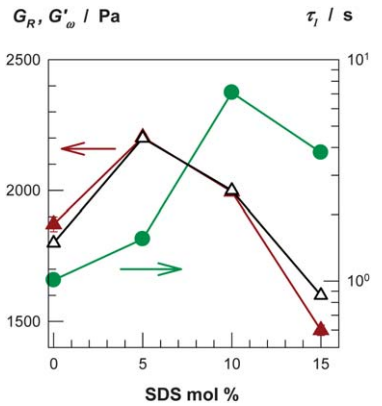

Fig. 5 Rouse modulus G_R (filled triangles), elastic modulus G'_ω at $\omega = 250$ rad s^{-1} (open triangles), and the lifetime τ_1 of hydrophobic associations in gels (filled circles), shown as a function of SDS content.

Rouse modulus G_R and the lifetime τ_1 derived from the fits are plotted in Fig. 5 against SDS %. The elastic moduli G'_ω of the gels at $\omega = 250$ rad s^{-1}, corresponding to an experimental time scale of 4 ms, are also shown in the figure. As the SDS content of gels is increased, that is, as the micelles grow bigger, the lifetime of the hydrophobic associations also increases while the limiting modulus G_R or G'_ω at short times decreases. These findings can be explained with the effect of the micellar size on the length of the hydrophobic blocks. Since the hydrophobe level is fixed in the experiments (2 mol%, except for the gels formed in CTAB solutions, which is 1.4 mol%), increasing size of the micelles also increases the number of C18 molecules solubilized in a given micelle so that longer hydrophobic blocks will form after polymerization but the number of blocks per primary polymer chain will decrease. This would increase the lifetime of the associations but decrease their concentration, as evidenced by the Rouse modulus of the physical gels. We note that the lower modulus of gels formed in the absence of SDS is attributed to the incomplete solubility of C18 in the reaction solution leading to the formation of a lesser amount of hydrophobic association in the final gels.

An experimental proof of this mechanism requires microstructural characterization of the network chains isolated from

the physical gels. However, all the physical gels were insoluble in water as well as in organic solvents. When put in a large excess of water, they swell and eventually attain equilibrium (relative) degrees of swelling around 4. Temporarily, the degree of swelling passes through a distinct maximum due to the large osmotic pressure of the enclosed ionic surfactants that are gradually extracted, as has been discussed in detail before[23] (Fig. S3‡). Gel fractions (mass of dry, extracted network/mass of the monomers in the comonomer feed) were close to 1 over the whole range of the SDS content studied confirming the existence of strong hydrophobic associations that are not destroyed during the expansion of the gel in water.

Although the physical gels were insoluble in water, they could easily be solubilized in aqueous 0.1–0.3 M SDS or CTAB solutions. These solutions exhibited low viscosities ($\sim 10^{-2}$ Pa s^{-1}) independent of the type of the gel, this fact being attributed to the weakening of the hydrophobic interactions due to the extensive number of surfactant micelles. Likewise, when swelling tests are conducted in a limited volume of water, *e.g.* 10 mL of water per 1 g of gel sample, complete dissolution of the physical gel takes place typically within several days. The surfactant concentration then drops to approx. 1/10 of the original one (24 mM), but this is still far above the cmc and the micelles provide for the temporary nature of the associations. These solutions containing 0.5 w/v% polymer also exhibited similar and low viscosities. Thus, the necessity of the presence of the surfactant micelles in the solutions prevents visualization of the blockiness of the network.

To gain insight into the extent of hydrophobic interactions inside the physical gels, they were dissolved in CTAB–SDS solutions at 35 °C having the same concentration (0.24 M) and composition (0 to 15% SDS) as those used for gel preparation. A surfactant solution of 10 mL volume was applied per 1 g of the gel sample so that the polymer concentration became 0.5 w/v%. In this way, we were able to solubilize the physical gels while the surfactant environment of the disintegrated network chains remained unchanged.

Fig. 6A presents the flow curves (viscosity *versus* shear rate) for 0.5 w/v% polymer solutions obtained from physical gels made with SDS contents between 0 and 15%. The solutions of polymers with 0 and 5% SDS show rather low viscosities, and those with 10 and 15% SDS exhibit higher viscosities at low shear rates and marked shear thinning. Since the increase in the viscosity with rising SDS content may be attributed to the micellar growth rather than to the increasing associativity of polymers, we also measured the viscosities of the surfactant solutions without the polymers (Fig. S4‡). The relative viscosity increase due to the polymer was represented as the specific viscosity η_{sp}, defined as:

$$\eta_{sp} = \frac{\eta_{o,polymer} - \eta_{o,solvent}}{\eta_{o,solvent}} \quad (4)$$

where $\eta_{o,polymer}$ and $\eta_{o,solvent}$ are the zero-shear viscosities of CTAB–SDS solutions with and without the polymers. The inset to Fig. 6A shows the specific viscosity η_{sp} of polymer solutions plotted against SDS content. η_{sp} rapidly increases with rising SDS content indicating increasing associativity of the network chains as the amount of SDS during the gel preparation is increased.

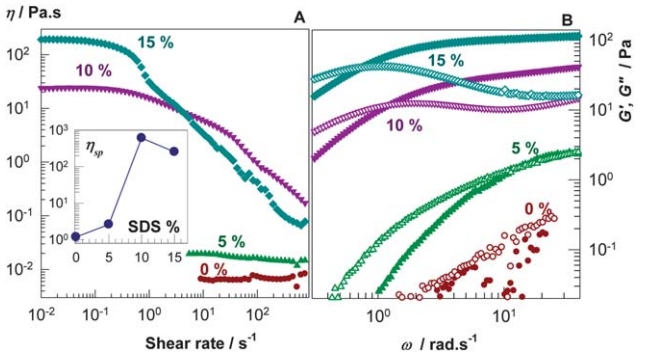

Fig. 6 Flow curves (viscosity *vs.* shear rate) (A) and frequency-sweeps (B) for the polymer solutions in 0.24 M surfactant solutions with various SDS contents indicated. In (B), G' and G'' are shown by the filled and open symbols, respectively. Polymer concentration = 0.5 w/v%. Inset to (A): specific viscosity η_{sp} of polymer solutions as a function of SDS content. Temperature = 35 °C.

The frequency-dependent G' and G'' for the polymer solutions are shown in Fig. 6B. The characteristic relaxation times τ_R, as determined by the crossover frequency ω_c where the G' and G'' curves intersect ($\tau_R = \omega_c^{-1}$), are 0.09, 0.83, and 1.3 s for SDS contents 5, 10, and 15 mol%, respectively. This also indicates increasing associativity of the network chains with rising amount of SDS in the gelation solutions. Fig. 6B also shows that at 5% SDS, a distinct plateau emerges in G' at high frequencies; the height of the plateau increases and its width expands with increasing SDS content. For instance, the plateau value of G' for the polymer solution with 15% SDS is two orders of magnitude higher than that with 5% SDS.

From these results, it is clear that the network chains formed in surfactant solutions with 10 and 15% SDS show remarkable associativity. We may attribute this to the pronounced blockiness of the network chains as well as to the increasing size of wormlike CTAB micelles surrounding the hydrophobic blocks.

Mechanical properties and self-healing behaviour

Tensile tests were conducted on cylindrical gel samples of various SDS contents. Although those formed at 0 and 5% SDS exhibited very high elongation ratios, they were too slippery to be measured accurately due to the sample slippage from or breakage at the grip. Fig. 7A represents tensile stress–strain data of the physical gels formed at 10 and 15% SDS. Increasing amount of SDS decreases the elongation ratio at break from 5000 ± 300% to 1800 ± 100%, while the ultimate strength increased from 6 to 10 kPa. This finding is in accordance with that of the previous section and confirms increasing associativity of the network chains. Moreover, as compared to the present hydrogels, those formed in SDS–NaCl solutions were too weak to obtain precise mechanical data even by use of a load cell of 10 N.[23]

The reversible dissociation–association of the cross-link zones in the gel network also provides self-healing property to the present hydrogels. As illustrated in Fig. 7B, when the fracture surfaces of ruptured gel samples are pressed together, the

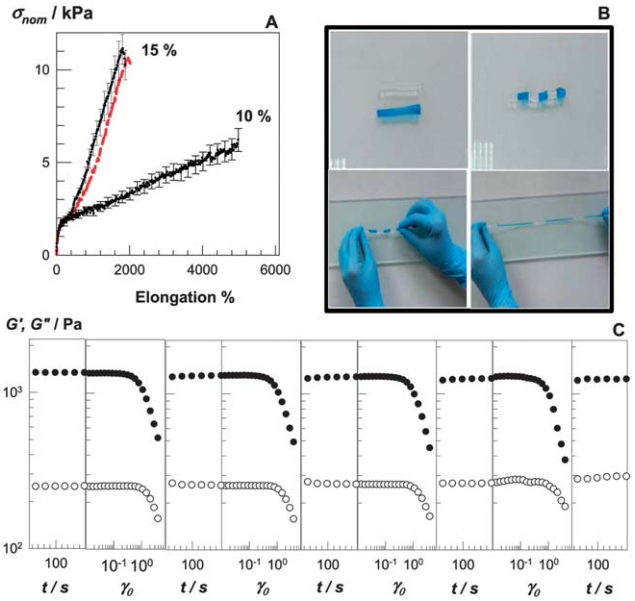

Fig. 7 (A): Stress–strain curves of the gels formed at 10 and 15% SDS. Standard deviations are shown as error bars. Temperature = 31.0 ± 0.5 °C. The dashed red curve represents the data of a healed gel sample formed at 15% SDS. (B): Photographs of two gel samples (one is colored with methylene blue for clarity) formed at 15 mol% SDS. After cutting into three pieces and pressing the fractured surfaces together for 3 min, they merge into a single piece. (C): Four successive time-sweeps at $\gamma_o = 0.01$ and strain-sweeps between $\gamma_o = 0.01$ and 4 conducted at 35 °C on a gel sample formed at 15% SDS. Duration between strain- and time-sweep tests is about 30 s. $\omega = 6.3$ rad s^{-1}.

pieces merge into a single piece. The joint reformed withstands very large extension ratios as the original gel sample before its fracture. The healing efficiency of the physical gels could be quantified using the gels formed at 15% SDS. The samples were cut in the middle and then, the two halves were merged together within a plastic syringe (of the same diameter as the gel sample) at 35 °C by slightly pressing the piston plunger. The healing time was set to 60 min and each experiment was carried out starting from a virgin sample. The dashed red curve in Fig. 7A represents typical stress–strain data of healed gel samples. An average healing efficiency of 98% was found using several gel samples. The healing behavior of gels was also demonstrated by oscillatory deformation tests. The gel samples were subjected to 4 successive time-sweep tests for 200 s at a strain amplitude of $\gamma_o = 0.01$ followed by strain-sweeps between $\gamma_o = 0.01$ and 4 (Fig. 7C). The dynamic moduli of all gels could be recovered after each cycle indicating that the damage done to the gel samples at large deformations is recoverable in nature.

Conclusions

Addition of SDS into an aqueous CTAB solution leads to the growth of the micelles and, hence, solubilization of the hydrophobic monomer C18 in the micellar solution. Copolymerization of AAm with 2 mol% C18 in these micellar solutions produces physical PAAm hydrogels with remarkable properties. The gels exhibit time-dependent dynamic moduli, high elongation ratios at break (1800–5000%), and self-healing, as evidenced by rheological and mechanical measurements and substantiated by DLS. As the size of the micelles in the gelation solution increases, both the degree of temporary spatial inhomogeneity and the lifetime of hydrophobic associations in gels increase while the elongation ratio at break decreases. Viscometric and rheological behaviors of the micellar solutions of polymers isolated from the gels show, in parallel with micellar growth, a substantial increase in the associativity of the network chains that result in prolonged lifetime of hydrophobic associations acting as physical cross-links in gels. The internal dynamics of self-healing gels could thus be controlled by the associativity of the network chains which in turn depends on the size of CTAB micelles.

As compared to the present hydrogels, those formed in solutions of grown SDS micelles were much weaker,[23] indicating that replacement of SDS–NaCl with a CTAB–SDS mixed micellar system further improves the mechanical performance of self-healing hydrogels. For instance, both G' and G'' of the gel formed in an SDS solution are congruent and show power-law behavior, $G' \propto \omega^{0.47}$ and $G'' \propto \omega^{0.44}$, suggesting that it is close to the critical gel state possessing self-similar fractal structure over a wide spatial scale.[23] In contrast, the elastic modulus of the present gel formed in a catanionic micellar solution is much larger than the viscous modulus over the whole frequency range investigated indicating that the present gels are more elastic than those formed in SDS micelles. This difference is attributed to the fact that CTAB is more hydrophobic due to its longer alkyl chain length as compared to SDS contributing the extent of hydrophobic interactions between C18 blocks.

Acknowledgements

This work was supported by the Scientific and Technical Research Council of Turkey (TUBITAK) and International Bureau of the Federal Ministry of Education and Research of Germany (BMBF), TBAG – 109T646. O. O. thanks Turkish Academy of Sciences (TUBA) for the partial support.

Notes and references

1 I. Galaev and B. Mattiasson, *Smart Polymers. Applications in Biotechnology and Biomedicine*, 2nd edn; CRC Press, Taylor & Francis Group, Boca Raton, 2008.
2 A. Ahagon and A. N. Gent, *J. Polym. Sci., Polym. Phys. Ed.*, 1975, **13**, 1903–1911.
3 H. R. Brown, *Macromolecules*, 2007, **40**, 3815–3818.
4 G. E. Fantner, E. Oroudjev, G. Schitter, L. S. Golde, P. Thurner, M. M. Finch, P. Turner, T. Gutsmann, D. E. Morse, H. Hansma and P. K. Hansma, *Biophys. J.*, 2006, **90**, 1411–1418.
5 S. Mora, *Soft Matter*, 2011, **7**, 4908–4917.
6 V. Amendola and M. Meneghetti, *Nanoscale*, 2009, **1**, 74–88.
7 P. J. Skrzeszewska, J. Sprakel, F. A. Wolf, R. Fokkink, M. A. C. Stuart and J. van de Gucht, *Macromolecules*, 2010, **43**, 3542–3548.
8 Z. Rao, M. Inou, M. Matsuda and T. Taguchi, *Colloids Surf., B*, 2011, **82**, 196–202.

9 S. Seiffert and J. Sprakel, *Chem. Soc. Rev.*, 2012, **41**, 909–930.
10 S. Abdurrahmanoglu, V. Can and O. Okay, *Polymer*, 2009, **50**, 5449–5455.
11 P. Cordier, F. Tournilhac, C. Souli-Ziakovic and L. Leibler, *Nature*, 2008, **451**, 977–980.
12 J. Canadell, H. Goossens and B. Klumperman, *Macromolecules*, 2011, **44**, 2536–2541.
13 J. P. Gong, Y. Katsuyama, T. Kurokawa and Y. Osada, *Adv. Mater.*, 2003, **15**, 1155–1158.
14 Y. Tanaka, J. P. Gong and Y. Osada, *Prog. Polym. Sci.*, 2005, **30**, 1–9.
15 Y. Okumura and K. Ito, *Adv. Mater.*, 2001, **13**, 485–487.
16 G. Miquelard-Garnier, S. Demoures, C. Creton and D. Hourdet, *Macromolecules*, 2006, **39**, 8128–8139.
17 K. Haraguchi and T. Takehisa, *Adv. Mater.*, 2002, **14**, 1120–1124.
18 T. Huang, H. Xu, K. Jiao, L. Zhu, H. R. Brown and H. Wang, *Adv. Mater.*, 2007, **19**, 1622–1626.
19 G. Deng, C. Tang, F. Li, H. Jiang and Y. Chen, *Macromolecules*, 2010, **43**, 1191–1194.
20 J. Hao and R. A. Weiss, *Macromolecules*, 2011, **44**, 9390–9398.
21 F. Liu, F. Li, G. Deng, Y. Chen, B. Zhang, J. Zhang and C.-Y. Liu, *Macromolecules*, 2012, **45**, 1636–1645.
22 Q. Wang, J. L. Mynar, M. Yoshida, E. Lee, M. Lee, K. Okuro, K. Kinbara and T. Aida, *Nature*, 2010, **463**, 339–343.
23 D. C. Tuncaboylu, M. Sari, W. Oppermann and O. Okay, *Macromolecules*, 2011, **44**, 4997–5005.
24 H. Rehage and H. Hoffman, *Mol. Phys.*, 1991, **74**, 933–973.
25 P. J. Missel, N. A. Mazer, G. B. Benedek and C. Y. Young, *J. Phys. Chem.*, 1980, **84**, 1044–1057.
26 L. J. Magid, *J. Phys. Chem. B*, 1998, **102**, 4064–4074.
27 F. Candau and J. Selb, *Adv. Colloid Interface Sci.*, 1999, **79**, 149–172.
28 E. Volpert, J. Selb and F. Candau, *Polymer*, 1998, **39**, 1025–1033.
29 A. Hill, F. Candau and J. Selb, *Macromolecules*, 1993, **26**, 4521–4532.
30 E. J. Regalado, J. Selb and F. Candau, *Macromolecules*, 1999, **32**, 8580–8588.
31 F. Candau, E. J. Regalado and J. Selb, *Macromolecules*, 1998, **31**, 5550–5552.
32 P. Kujawa, A. Audibert-Hayet, J. Selb and F. Candau, *J. Polym. Sci., Part B: Polym. Phys.*, 2004, **42**, 1640–1655.
33 P. Kujawa, A. Audibert-Hayet, J. Selb and F. Candau, *Macromolecules*, 2006, **39**, 384–392.
34 D. C. Tuncaboylu, M. Sahin, A. Argun, W. Oppermann and O. Okay, *Macromolecules*, 2012, **45**, 1991–2000.
35 K. L. Herrington, E. W. Kaler, D. D. Miller, J. A. Zasadzinski and S. Chiruvolu, *J. Phys. Chem.*, 1993, **97**, 13792–13802.
36 P. A. Hassan, T. K. Hodgdon, M. Sagasaki, G. Fritz-Popovski and E. W. Kaler, *C. R. Chim.*, 2009, **12**, 18–29.
37 F. Geng, L. Yu, Q. Cao, Z. Li, L. Zheng, J. Xiao, H. Chen and Z. Cao, *J. Dispersion Sci. Technol.*, 2009, **30**, 92–103.
38 W. Brown, K. Johansson and M. Almgren, *J. Phys. Chem.*, 1989, **93**, 5888–5894.
39 P. Koshy, V. K. Aswal, M. Venkatesh and P. A. Hassan, *Soft Matter*, 2011, **7**, 4778–4786.
40 E. Feitosa and W. Brown, *Langmuir*, 1998, **14**, 4460–4465.
41 P. Koshy, G. Verma, V. K. Aswal, M. Venkatesh and P. A. Hassan, *J. Phys. Chem. B*, 2010, **114**, 10462–10470.
42 M. Törnblom, U. Henriksson and M. Ginley, *J. Phys. Chem.*, 1994, **98**, 7041–7051.
43 F. Wang, T. Chen, Y. Shang and H. Liu, *Korean J. Chem. Eng.*, 2011, **28**, 923–926.
44 S. Zhang and H. N. Teng, *Colloid J.*, 2008, **70**, 105–111.
45 B. Tah, P. Pal, M. Mahato and G. B. Talapatra, *J. Phys. Chem. B*, 2011, **115**, 8493–8499.
46 K. Beyer, D. Leine and A. Blume, *Colloids Surf., B*, 2006, **49**, 31–39.
47 J. G. H. Joosten, J. L. Mccarthy and P. N. Pusey, *Macromolecules*, 1991, **24**, 6690–6699.
48 P. N. Pusey and W. van Megen, *Physica A*, 1989, **157**, 705–741.
49 F. Ikkai and M. Shibayama, *Phys. Rev. Lett.*, 1999, **82**, 4946–4949.
50 S. Förster, M. Schmidt and M. Antonietti, *Polymer*, 1990, **31**, 781–792.
51 V. S. Molchanov, O. E. Philippova, A. R. Khokhlov, Y. A. Kovalev and A. I. Kuklin, *Langmuir*, 2007, **23**, 105–111.
52 S. Kumar, D. Bansal and K. Din, *Langmuir*, 1999, **15**, 4960–4965.
53 H. Kunieda, K. Ozawa and K.-L. Huang, *J. Phys. Chem. B*, 1998, **102**, 831–838.
54 W. Siriwatwechakul, T. LaFleur, R. K. Prud'homme and P. Sullivan, *Langmuir*, 2004, **20**, 8970–8974.
55 T. Sato, D. P. Acharya, M. Kaneko, K. Aramaki, Y. Singh, M. Ishitobi and H. J. Kunieda, *J. Dispersion Sci. Technol.*, 2006, **27**, 611–616.
56 G. Williams and D. C. Watts, *Trans. Faraday Soc.*, 1970, **66**, 80–88.
57 A. A. Gurtovenko and Y. Y. Gotlib, *J. Chem. Phys.*, 2001, **115**, 6785–6793.
58 T. S. K. Ng and G. H. McKinley, *J. Rheol.*, 2008, **52**, 417–449.